A series of bisamide-substituted diacetylenes exhibiting terminal alkyl odd-even parity effect on mechano-activation for the subsequent photopolymerization property

Jiajun Qi,[a]# Yuna Kim,[a]# Kiyonori Takahashi,[a] Ken'ichi Aoki,[b] Ichiro Hisaki,[c] Takayoshi Nakamura,[a] and Nobuyuki Tamaoki*[a]

[a] Mr. J. Qi, Dr. Y. Kim, Dr. K. Takahashi, Prof. Dr. T. Nakamura, Prof. Dr. N. Tamaoki
Research Institute for Electronic Science
Hokkaido University
N20, W10, Kita-Ku, Sapporo, 001-0020, Japan
E-mail: tamaoki@es.hokudai.ac.jp
[b] Dr. K. Aoki
Department of Chemistry, Graduate School of Science, Faculty of Science
Tokyo University of Science
1-3 Kagurazaka, Shinjuku-ku, Tokyo, 162-8601, Japan
[c] Prof. Dr. I. Hisaki
Graduate School of Engineering Science
Osaka University
1-3, Machikaneyama, Toyonaka, Osaka, 560-8531, Japan
# Jiajun Qi and Yuna Kim contributed equally to this work.

Supporting information for this article is given via a link at the end of the document.

Abstract: Diacetylene derivatives exhibit solid-state polymerization to polydiacetylene initiated by UV light or γ-ray irradiation. The activation of the photopolymerization highly relies on the monomer diynes arrangement. Recently, we have demonstrated the first mechanoresponsive bisamide substituted diacetylenes (DAs) showing dramatic switching from light-inert to light-reactive state upon a given pressure. The origin of this unique phenomenon was apparently related to the pressure-sensitive crystalline transition in DAs, but the molecular mechanism remains elusive. To obtain the insight, we herein present a series of DAs with varying terminal alkyl spacer length, and their molecular structural effect on the intermolecular hydrogen bonding and steric repulsion. In pristine states, even-parity DAs were inactive upon UV irradiation (λ=254 nm) unless external pressure was given. By contrast, odd-parity DAs were easily polymerized upon UV irradiation without pressure application. However, the pressure-induced crystalline phase transition exhibiting photopolymerization was valid for all DAs regardless of their alkyl spacer length. A systematic investigation revealed that the terminal alkyl spacer length, especially its odd-even parity plays a key role to determine the intrinsic intermolecular hydrogen bonding nature of DA crystals and resultant molecular packing. In addition, the relevant thermochromic behaviour was also observed from photopolymerized polydiacetylenes.

Introduction

Mechanochemical transduction using mechanophores has been widely utilized to exploit mechanical energy for stress-sensing, imaging, patterning, and the synthesis of functional polymers.[1-6] From this perspective, diacetylenes (DAs) are one of the promising transducers as the transitions in intermolecular interactions and molecular packings result in a significantly different polymerization behavior. DA derivatives usually can undergo solid-state polymerization initiated by UV or γ-ray irradiation, and the arrangement of monomeric diynes is a key for the activation of such photochemical process. In order to form ideally conjugated polydiacetylene (PDA) under 1,4-polymerization, DA should orient at a translational repeat distance matching the polymer repeat unit (~4.9 Å) with a tilt angle of around 45°, having C1 of one monomer to within van der Waals distance (~3.5 Å) of C4 in the neighboring monomer.[7-12] Well-organized PDAs are likely to show intense blue color because of electron delocalization in the linear π-conjugation. Although mechanoresponsive chromatic properties in PDAs have been well known and studied, mechanical tuning of monomeric DA arrangements and so as derived control its photopolymerizability has been scarcely reported.[11-13]

Recently, our group has succeeded to showcase DA derivatives which can undergo an unprecedented phase transition from light-inert to the light-reactive state by mechanical pressure.[13] Introducing bisamide groups to DA molecules brought intermolecular hydrogen bonding which benefited monomeric assembly to enable selective photopolymerization in crystals. Even with a small pressure application to the bisamide substituted DA derivatives (at a minimum force of 2 MPa), it resulted in the phase transition from unfavorable to favorable crystalline state to undergo photo-induced topochemical polymerization of bulk DA crystals. This mechanoresponsive monomeric DA crystal could provide an effective methodology to a mechanically tunable "on-demand" formation of the conjugated polymer.

To obtain such pressure-addressed photosensitivity, achieving an initial light-inert crystalline state is essential. In terms of molecular structure engineering, intrinsic topochemical polymerization behaviour of diacetylenes depending on

functional groups or odd/even parity of alkyl spacers has been extensively studied.[14-18] Structural manipulations to DAs such as implementing symmetric/asymmetric hydrogen bonds[14] and modulating bulky aromatic groups[15] or alkyl spacers[15-18] have been investigated. However, to the best of our knowledge, its correlation to mechanoresponsive monomeric crystalline transition and the photopolymerization behaviour has never been studied.

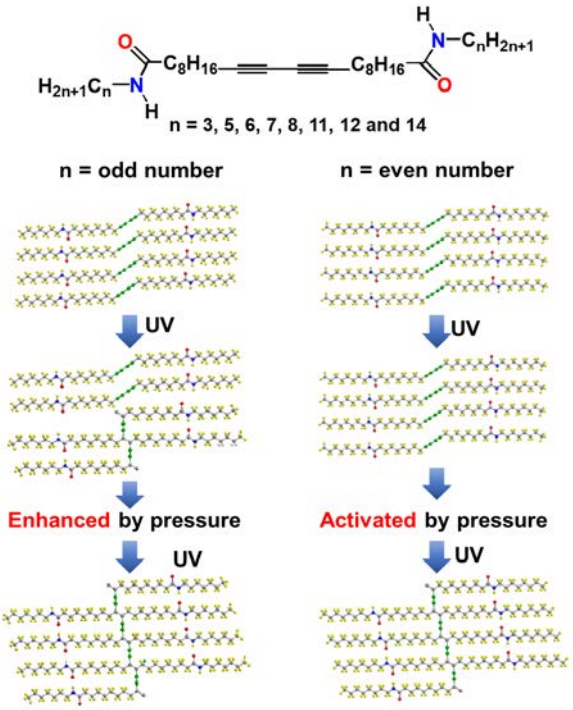

Scheme 1. Molecular structure of a series of bisamide-substituted diacetylene derivatives with terminal alkyl variations and their odd-even parity dependent mechano-photoresponsive properties.

Therefore, we herein systematically investigated the effect of the molecular structure of bisamide-substituted DAs for both intrinsic and pressure-induced photosensitivities by synthesizing DAs bearing different lengths of the terminal alkyl spacers connected to the amide units (Scheme 1). Surprisingly, in pristine states, even-parity DAs were inactive upon UV irradiation (λ = 254 nm) unless external pressure was given. By contrast, odd-parity DAs could easily polymerize upon UV irradiation without pressure application. Terminal alkyl odd/even parity and length influenced the intermolecular hydrogen bonding and steric repulsion which either facilitate or hinder the mechanical stimulus sensitivity and photopolymerization.

Controlling the odd-even parity of the alkyl spacer which directly connects the diacetylene group and the hydrogen-bonding generating functional group has been revealed to afford the most effective way for the molecular control of the photopolymerization properties of DA and thermochromic properties of PDA.[14-18] For example, odd-parity alkyl linker brought photopolymerization of DA derivatives while no polymerization was exhibited with even-parity alkyl linker.[18] The reversibility of thermochromic response was well contrasted by odd-even parity. Therefore, changing the odd-even parity or length of terminal alkyl spacer while sharing the identical core parts (*e.g.* amide-alkyl-diyene) has been less highlighted to date. However, the synthesis of those series of DA derivatives is time-consuming and expensive. Because it should start from constructing each building block bearing different alkyls adjacent to the diacetylene unit. In this study, we demonstrate that the photopolymerization ability of DAs can be rather simply tuned by changing terminal alkyl length which would considerably save the effort and expense of synthesizing a series of DAs for different purposes that are selectively responsive to either pressure or light. In addition, we confirmed the stable thermochromic behavior of bisamide-substituted PDAs switching between blue, purple, red and orange phases which allows its application for patternable temperature sensors.[19]

Results and Discussion

Photo- and mechanical pressure-response of pristine DA crystals

DAs exhibiting unique topochemical polymerization behavior consist of three parts- a diacetylene group, bisamide group connected to diacetylene unit by octyl spacers, and the series of different terminal alkyl chains. The number of methylene units (n) of the terminal spacer are varied as n = 3, 5, 6, 7, 8, 11, 12 and 14 (Scheme 1). Their synthesis and structural analysis are described in the Experimental Section. Before use, most light-inert monomeric crystals were prepared by recrystallization in methyl ethyl ketone (MEK) referred to our previous report.[13]

Table 1. Photos of DA crystal powders showing responsiveness to light (UV irradiation at 254 nm for 2 min) and/or mechanical pressure (pressured at 50 MPa).

	Entry	n = 3	n = 5	n = 6	n = 7	n = 8	n = 11	n = 12	n = 14
a)	pressure × ↓ UV ×								
b)	pressure ○ ↓ UV ×	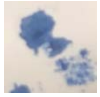							
c)	pressure × ↓ UV ○								

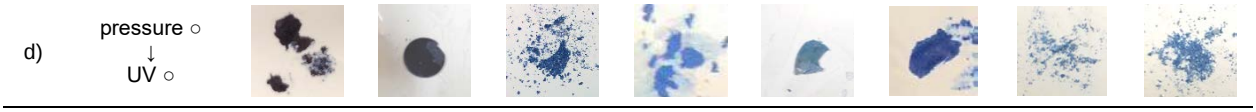

[a]Pristine powder state; [b]pressured state; [c]UV light irradiated state; [d]UV irradiated state after pressured.

Table 1 depicts topochemical polymerization characteristics of each DA derivative towards UV light (254 nm light with handheld UV lamp) and mechanical pressure. Interestingly, we witnessed clearly different photosensitivity of DA derivatives in pristine (0 MPa) and pressured (50 MPa) states depending on their terminal alkyl length as well as odd/even parity. Pristine crystal powders obtained from DAs with even-parity, n = 6, 8, 12 and 14 exhibited totally light-inert state upon UV light irradiation maintaining the white monomeric states. After pressing the pristine powders followed by irradiating UV light, blue colored PDAs were observed which implies that the topochemical polymerization of monomeric DA to PDA proceeded as the result of 1,4-addition reactions of the diyne groups. Those DA crystalline states after pressurization were quite stable maintaining the photosensitivity for a year as far as we have confirmed. In terms of reversibility, MEK vapor exposure to pressured DAs could somewhat reverse the crystalline states to partially light-inert state. Whereas, pristine powders obtained from DAs with odd-parity n = 3, 5, 7 and 11 showed instant color transition from white to blue upon UV irradiation indicating photopolymerization could proceed which is different from even-parity DAs. In the meantime, odd-parity DAs showed partial color transition from white to blue by pressurization even without photoirradiation implying their favorable molecular arrangements for topochemical polymerization. By shortening the terminal alkyl length to n=3, even the spontaneous polymerization occurred showing color transition from white to blue at dark condition during drying in vacuum after recrystallization. Subsequent UV irradiation resulted in entire color transition to darker blue meaning further photopolymerization could proceed.

Hydrogen bonding characterization of DAs at pristine state and pressure-induced crystalline transition state

To understand the origin of such differences in photoactivity of DA crystals, analysis using Fourier transform infrared (FT-IR) spectroscopy by the attenuated total reflection (ATR) method and X-ray diffraction (XRD) was carried out. FT-IR spectra feature intermolecular hydrogen bonding characteristics formed in the DA pristine crystals depending on their odd-even parity and length of terminal alkyl (Figure 1). Intrinsic intermolecular hydrogen bonds in DA crystals between the secondary amide moieties were confirmed at ca. 3290 ~ 3340, 1633, and 1500 ~ 1550 cm^{-1} which are assigned to ν_{NH}, $\nu_{C=O}$ (amide-I), and δ_{NH} (amide-II) bands, respectively. The absence of free N-H stretching at 3440 cm^{-1} reflects that the amide units were fully hydrogen-bonded in all DA derivatives. Most noticeable variations were observed regarding ν_{NH} at around 3326 ~ 3337 cm^{-1}. DAs of even-parity show distinctive single band, while those of odd-parity show intense and red-shifted ν_{NH} to lower wavenumber at around 3290 cm^{-1} with much diminished stretchings in 3326 ~ 3333 cm^{-1}. In particular, the shortest DA n=3 shows only N-H stretching in lower wavenumber at 3290 cm^{-1}. In terms of amide II bending, even-parity DAs show the bands centered at 1523 cm^{-1} while odd-parity DAs show rather broadened ones at higher wavenumber. Difference in odd-even parity for $\nu_{C=O}$ (amide I) stretching at around 1633 cm^{-1} was less pronounced than that of amide-II, but still odd-parity DA stretchings positioned at slightly lower wavenumber than those of even-parity. Based on those observations, we could speculate that stronger hydrogen bonds exist with odd-parity DAs than even-parity ones. Consequently, a clear tendency was witnessed between the degree of hydrogen bonding and the photosensitivity of each DA derivative in pristine state. As the terminal alkyl spacer elongates with even parity forming the weaker intermolecular H-bonds, DA crystal exhibits totally light-inert pristine state. By contrast, DA with odd-parity terminal alkyls affording rather strong intermolecular H-bonds exhibits high photosensitivity in pristine state undergoing photopolymerization upon UV light exposure. Decreasing steric repulsion of neighboring alkyl chains led to the strongest H-bond for DA n=3 which enabled spontaneous topochemical polymerization without light or mechanical stimulus. Meanwhile, upon pressure (50 MPa) application to each DA, stretchings related to intermolecular H-bond exhibited transitions such as evolved stretchings 3294 ~ 3300 cm^{-1} (Figure S1). We have reported the emergence of the new band at lower wavenumber with DA n=8 and n=14 by pressure application.[13] By increasing the applied force, more pronounced new band was observed. The newly synthesized even-parity DA n=6 and n=12 also showed these bands at similar wavenumber region after 50 MPa application. Therefore, the pressure-induced strengthening of H-bonds was well distinguishable with even-parity DAs. In case of odd-parity DAs, some extent of deformation in crystal packing occurred upon pressure application, but it less affected major intermolecular hydrogen-bonding characteristics of DA crystals due to the relatively strong H-bonds in pristine states. The relative orientation of DAs may become denser mainly due to the adjustment of diacetylene part (π-π stacking) while maintaining the intrinsic hydrogen bonding to complement the volume decrease of the unit cell against the applied force.[13,20]

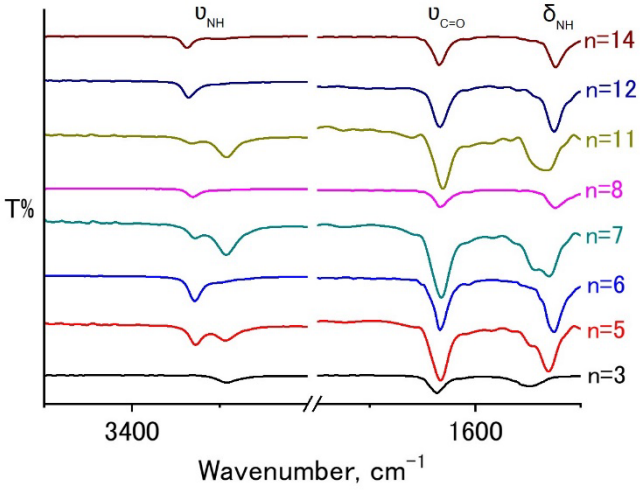

Figure 1. FT-IR spectra of DA crystals in pristine states.

A series of powder XRD patterns of pristine DAs (Figure S2) showed intense and sharp peaks indicating the crystalline aggregates were well ordered. Distinctive features at equidistant positions were much dominant in low-angle peaks than those in wide-angles. Relatively intense and multiple sharp wide-angle peaks (at 2

theta of 15 ~ 25°) were observed for DAs with shorter terminal alkyls, most distinctive in DA n=3 which was spontaneously polymerized even in pristine state. Figure 2 representatively demonstrates the transition of XRD patterns of DA n = 6, 7, 11 and 12 upon the application of mechanical pressure. The emergence of several new peaks and the shift of peak positions were shown in the diffraction patterns after pressured at 50 MPa reflecting the crystal phase transition occurred in a wide range as witnessed. In the low- angle region, only slight peak position shift as well as arise of some peaks has been observed around 4 ~ 5° assigned to (003) plane, from which we calculated *c*-axis lattice constants as 33.86, 35.14, 43.10 and 44.30 Å for DAs n = 6, 7, 11 and 12, respectively, suggesting minor lamellar phase crystal structure transition in (00n) phases. In particular, regardless of the terminal alkyl length of DAs, the peaks in the wide-angles in 15 ~ 25° exhibited the distinctive transitions corresponding to the *d*-spacings of 4.47 ~ 3.46 Å. This implies that the polymerization-favorable molecular orientations within the intermolecular distances (3.5 ~ 5.0 Å) were prompted by pressure in both even and odd-parity DAs. Enhanced reactivity was enough to result in either pressure or photo-induced topochemical polymerization for odd-parity DA n = 7 and 11 while it activated the photopolymerizability for even-parity DA n = 6 and 12 (XRD patterns of DA n=5 shown in Figure S3).

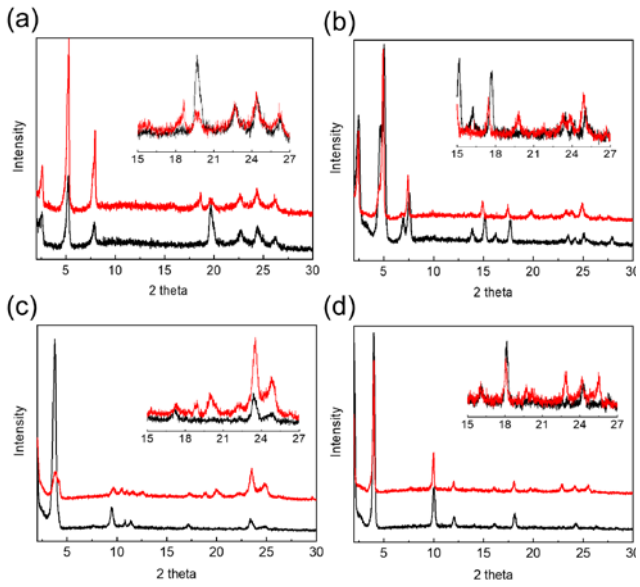

Figure 2. Powder XRD patterns of DAs before (black) and after the pressure application (red) at 50 MPa: (a) n=6, (b) n=7, (c) n=11, and (d) n=12. Insets are magnified peaks in the region of 20 ~ 25°.

Fortunately, we could isolate the single crystal and succeed to observe the molecular arrangement of DA n=8 from X-Ray crystallography (Crystallographic data summarized in Table S1 and Figure S4). DA n=8 was crystallized with triclinic *P*-1 space group. Half molecule is crystallographically independent. Figure 3a and 3b summarize the packing structure of DA n=8. Although molecule of DA n=8 is expanded to 48.553 Å long between terminal carbon•••carbon atoms, the *c* axis of unit cell is 36.455 Å because average plane of DA n=8 is tilted 44.73° with respect to the (001) plane. As shown in Figure 3a, O=C-N-H amide groups in both sides of DA n=8 are interacted to DA n=8 molecule by N-H•••O hydrogen bonding (N•••O distance and N-H•••O angles are 3.036 Å and 166.62°, respectively, classified as moderate hydrogen bonding[21]). This N-H•••O hydrogen bonds are elongated to (100) direction, forming one-dimensional hydrogen bonding chain along the *a* axis. Molecules are one-dimensionally arranged along the *a* axis by two N-H•••O hydrogen bonding chains (Figure 3a). This one-dimensional arrangement is stacked along the *b* axis, forming three-dimensional packing structure (Figure 3b).

According to the reference[22], necessary (but not sufficient) conditions for the topochemical reaction to occur are as follows: (i) the distance between possibly reacting terminal acetylenic carbon atoms in neighboring molecules (R_v) in the range of 3.4 ~ 4 Å; (ii) the angle γ between the DA rod and the translational vector favorably close to 45º; (iii) the distance (*d*) of monomer-monomer separation in the range around 4.4 ~ 5.6 Å (upper limit varies 5.2 ~ 5.6 Å depending on R_v and γ). As shown in Figure 3c, one molecule has two types of neighboring molecules with/without hydrogen bonding, which were assigned as **A** and **C** for **B**, respectively. From the crystal structure, *d*, R_v and γ defined above was 5.508 (9) Å, 3.771 (8) Å, and 43.1 (1)° between alkylamidediyne of **A** and **B**. All three parameters were in the range for topochemical reaction, while *d* was slightly at the inactive-reactive border in the grey zone. Between **B** and **C**, *d*, R_v and γ were 5.148 (8) Å, 5.148 (8) Å and 89.02°, which were out of range for topochemical reaction. We could confirm no topochemical reaction in DA n=8 single crystals at ambient pressure which implies that those three conditions necessary to be satisfied for polymerization are quite close to the border, but slightly out of the range for topochemical reaction. Although it was impossible to obtain the molecular arrangement of this single crystal after pressure application by X-Ray crystallography, comparison of its XRD pattern with powder XRD pattern of DA n=8 bulk crystals pressed at 50 MPa showed the small transition in (00n) planes while different planes were observed in the wide-angles in 18 ~ 27° (Figure S5). (001) plane *d*-spacing of bulk crystals was changed from 37.15 Å to 36.05 Å by pressure while that of single crystal was 36.46 Å implying the pressure-induced transition in the *c*-axis of a unit cell. In addition, as *d*-spacing of (010) plane at 18.68° is proportional to *d*, the associated peaks in powder XRD patterns of pristine DAs and pressed DAs from our previous report[13] could be assigned to show shorter *d*-spacings at a wider angle of 19.26° and a new peak at 19.87°, respectively. This also suggests that DA n=8 single crystals have unfavorable arrangement for polymerization at first and can change to have favorable arrangement for polymerization by pressuring. Although we failed to analyze the packing structure of the odd-parity DA single crystals, similar long-range lamellar packing can be speculated considering the similar XRD patterns observed in low-angle regions of DA n=7 (Figure 2b) and DA n=8 (Figure S5), but parameters (*d*, *Rv* and γ) could plausibly be within the range for topochemical reaction for DA n=7.

The geometric differences at the molecular level have a critical effect on the bulk photopolymerization properties. The initial crystal packing geometries and morphologies of some DA derivatives are known to be determined by the odd-even parity of the alkyl spacers affecting the orientation of H-bonded units.[23] Our elaborated results from FT-IR, XRD and X-ray single crystal analysis also provide the understanding on the cooperative effect of amide groups and terminal alkyl chains in DAs to the molecular packing modes. The secondary amide units at both sides of neighboring molecules become fixed through the formation of intermolecular hydrogen bonds. The odd-parity alkyls are likely to satisfy the molecular packing geometries enabling photopolymerization through strong hydrogen bonds in pristine state while even-parity alkyls have steric repulsion resulting in unfavorable packing geometries for photopolymerization and relatively weaker intermolecular hydrogen bonds.

Differential scanning calorimetry (DSC) analysis could provide further insight into the pressure-induced crystalline phase transformations and their thermal properties (Figure 4 and S6). The DSC thermograms in each first heating and cooling cycle of DA n=11 (a,b) and n=12 (c,d), before (0 MPa) and after pressured at 50 MPa. It clearly shows changes in thermal phase transition temperatures (T_{peak}) along with ΔH between pristine and pressured states. Upon heating, endothermic peaks in the range of 80 and 100 °C were observed due to the Cr-Cr phase transition presumably resulting in the crystal phase exhibiting higher stability with photoactivity, where the pressured state had higher T_{peak} compared to those of pristine powders. Likewise, upon subsequent cooling from 110 °C which is below the melting temperature (around 123 °C), further shift of T_{peak} and the enthalpy differences were observed. It suggests that the different crystalline phases emerged by pressure which is a consistent phenomenon observed from our previous report on DA n=8 and n=14.[13] In addition, odd/even parity effect was also witnessed. Figure 4e and 4f feature the first T_{peak} depending on the terminal alkyl lengths of DAs upon heating and cooling, respectively. For heating process, systematic T_{peak} increase was observed by elongating the alkyl length for both even-parity and odd-parity DA series (Figure 4e).

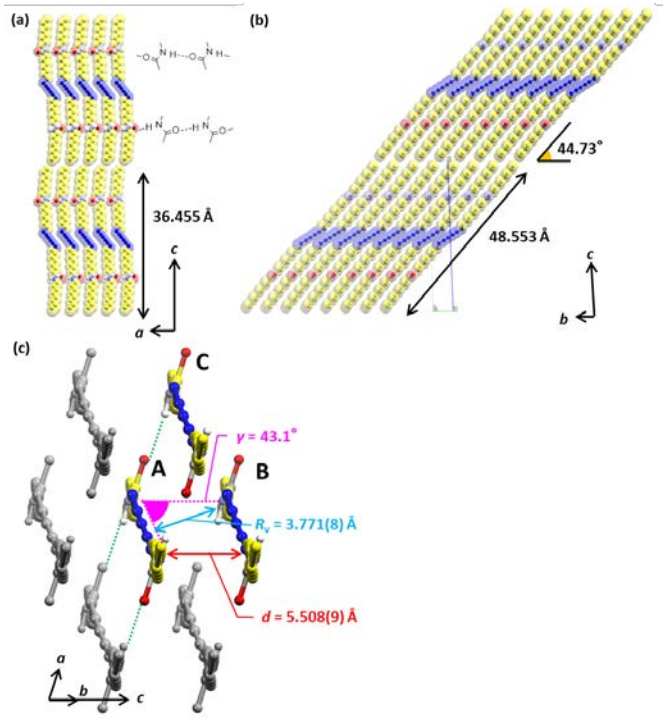

Figure 3. Molecular arrangement and structural evaluation for the topochemical reaction. Green lines correspond to hydrogen bonding. Blue and Yellow atoms belong to DA and alkylamide groups, respectively. Oxygen and nitrogen atoms are colored as red and white-blue, respectively. hydrogen atoms are omitted for clarity except the atoms involved in hydrogen bonding. (a, b) Packing structure viewed along with the (a) *b* and (b) *a* axes, respectively. Given values of 48.553 and 36.455 Å, and of 44.73° correspond to terminal carbon•••carbon distance of DA n=8 molecule, the c axis of the unit cell, and angles between (001) plane and averaged plane of DA n=8 molecule, respectively. (c) structural evaluation for the topochemical reaction. Details are described in the text.

Meanwhile at the cooling process, T_{peak} fluctuated according to the parity of terminal alkyl (Figure 4f). Overall, the odd-parity DAs exhibited higher phase transition temperatures compared to even-parity DAs. DA n=11 exhibited the highest T_{peak} among the studied samples implying the strong interactions within their crystalline domains attributable to the increment of dispersion interaction and/or strong hydrogen bonding nature confirmed in FT-IR (Figure 1). Every sample showed the shift of the T_{peak} upon pressure application (Figure 4 and S6) which indicates that they afford pressure-sensitive crystalline phase transitions, but the degree of T_{peak} shift was hardly relatable to the alkyl odd-even parity or the chain length.

Photopolymerization properties of DAs

Raman spectroscopy measurement (Figure 5) allowed us to verify the PDA formation from DA upon pressure and light exposure. Raman band at 2255 cm^{-1} indicating purely monomeric C≡C bonds appeared for all DAs except n=3 at each initial state. UV light irradiation and/or pressure application onto pristine DAs resulted in the obvious contrast in the Raman spectra depending on the terminal alkyl parity. Upon UV light irradiation onto pristine DAs (spectra for "0 MPa + UV"), odd-parity DAs exhibited drastic reduction of the monomeric C≡C band at 2255 cm^{-1} while new bands at 1445 and 2078 cm^{-1} are assignable to the conjugated C=C bond and C≡C bond of PDA, respectively. Notably, even-parity DAs showed the unchanged spectra because of totally light-inert initial crystalline states. Then, the dramatic transition from "totally light-inert state" to "photopolymerizable state" was confirmed for even-parity DAs by the UV light irradiation to the pressured DAs at 50 MPa (spectra for "50 MPa + UV") exhibiting two new bands at 1445 and 2078 cm^{-1} corresponding to the generation of PDAs. By contrast, odd-parity DAs pressed to 50 MPa underwent spontaneous blue PDA formation (spectra for "50 MPa") showing conjugated C=C and C≡C bands ascribed to the topochemical polymerization at moderate pressure. Considering even-parity DAs rarely showed such pressure-induced polymerizability, odd-parity DAs would have lower activation energy favorable for the polymerization photochemically and mechanically.

PDA color transition behavior upon thermal stimuli

Furthermore, we studied the color transition behavior of PDAs upon thermal treatment (thermochromism) which were formed by the photo-induced 1,4-addition reactions of the diyne groups. The color transition of PDAs is typically caused by changing the distortion degree of the conjugated ene-yne chains in PDAs.[8-10,24] Various blue-red color transition temperatures and reversibility have been reported from H-bond incorporated PDA derivatives.[14,24-26] We increased the temperature (10 °C/min) and maintained for one minute at certain temperatures while measuring the spectra.

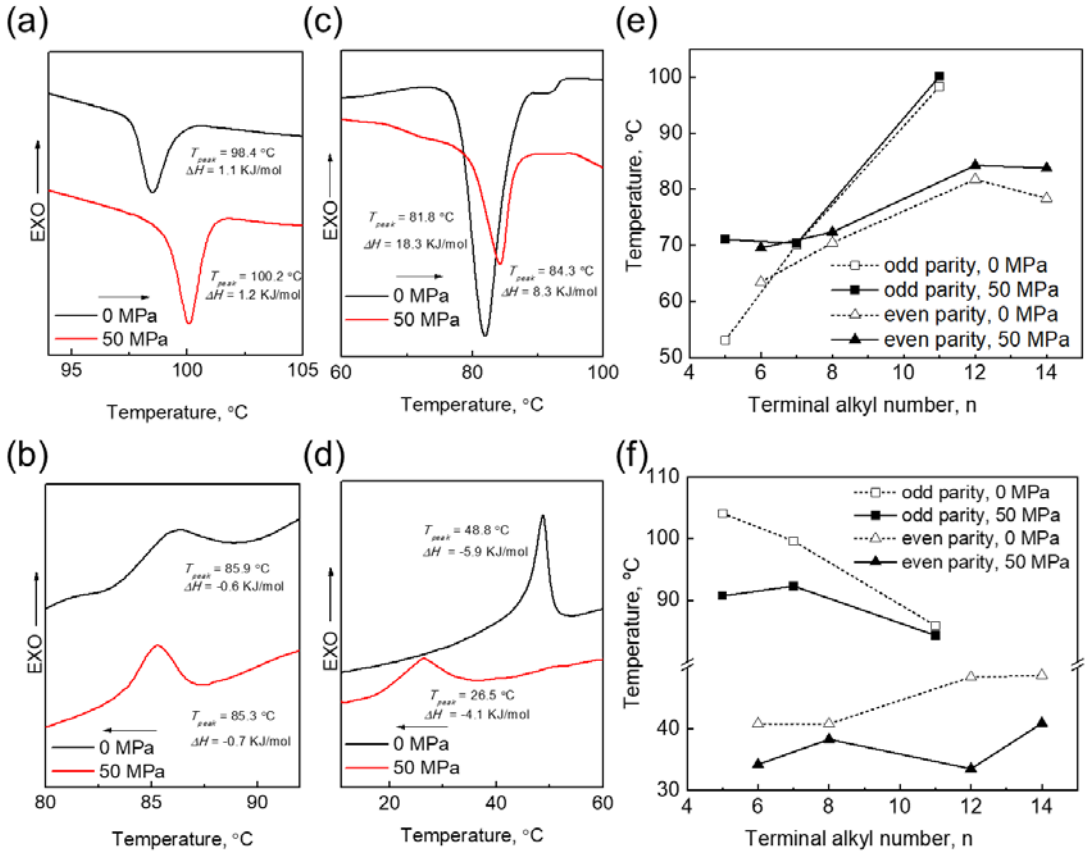

Figure 4. DSC results of DAs upon heating (top row) and cooling (bottom row). DSC traces of n=11 (a,b) and n=12 (c,d) at the first heating and cooling cycle at 2 °C/min. Plotting results of the first phase transition temperatures (T_{peak}) observed from DSC traces of DAs: (e) heating period and (f) cooling period.

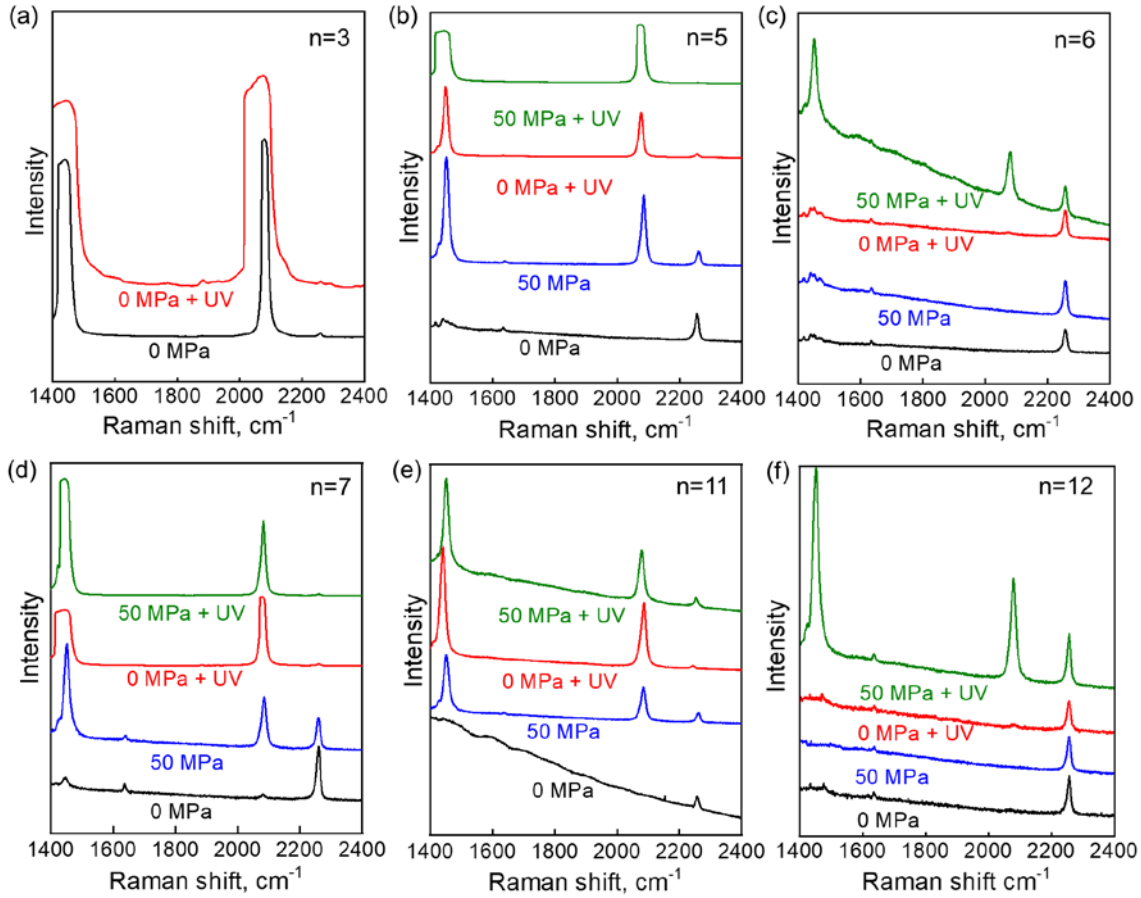

Figure 5. Raman spectra displaying topochemical polymerization behavior of DAs (a) n=3, (b) n=5, (c) n=6, (d) n=7, (e) n=11, and (f) n=12 of pristine state (0 MPa) and pressed state (50 MPa) without light exposure, and after UV light irradiation at 254 nm for 2 minutes at each state indicated as "0 MPa + UV" or "50 MPa + UV".

During heating process, PDA_{blue} exhibited the gradual color transition from blue to orange via purple and red for all PDAs in the temperature range from 75 ~ 100 °C to 130 °C as shown in Figure 6a. Upon subsequent cooling, they exhibited the decent color recovery of intermediate red and purple phases and finally returned to blue phase at room temperature. The reversible thermochromic behavior was confirmed from all PDAs upon repetitive heating and cooling cycles. UV-vis absorption spectra (Figure 6b~i) were measured with a reflective fiber type probe at each temperature. They feature the characteristic PDA bands with absorption maxima around 650 nm and 635 nm for odd- and even-parity PDA_{blue}, respectively, corresponding to the π-π* electronic transition with double bond vibronic coupling. Diamides in the odd-parity PDAs form extraordinary strong hydrogen bonding accommodated by the well positioned ene-yne backbone and brought rather red-shifted absorption bands. Subsequent thermal treatment to PDA_{blue} resulted in PDA_{red} phase with absorption maxima around 530 nm. Although all samples showed blue-shift of absorption maxima at 80 °C, PDAs with elongated even-parity chains such as n = 8, 12 and 14 showed apparently lower absorption shoulder at 614 nm, and sharp absorption decrease in the wavelength beyond the absorption maxima at 130°C exhibiting pure orange color reflecting the relatively flexible thermal fluctuations in conjugated channels among a series of PDAs (Figure S7). Upon cooling from 130 °C, all PDAs exhibited red-shift of absorption band and showed high reversibility of initial bands at 25 °C. In contrast, PDAs containing two amide groups linked by central odd- or even-alkyl spacers have been reported to exhibit irreversible or reversible thermochromism, respectively.[14] Therefore, the parity between amide groups may affect the reversibility and in case of our series of PDAs, bearing identical "DA-even-chain-amide" core would contribute to the similar reversible thermochromism. Meanwhile, the extension of mid or terminal alkyl spacer lengths in PDA derivatives has been reported to exhibit color transition in a wider temperature range of 10 ~ 30 °C, and the shift of absorption bands varied 50 ~ 100 nm.[25,26] Our PDA thermochromism showed 100 ~ 125 nm spectral shift which is comparable to previous reports. In addition, at "blue to purple" and "purple to red" color transitions, around 10 ~ 20 °C higher transition temperatures were observed from odd-parity PDAs compared to those of even-parity. It implies that odd-parity PDAs have more stable structures than even-parity PDAs, and consequently, the terminal alkyl parity influenced the polymerized packing states and conjugation chain distortion degrees upon thermal stimulus. The cooperative effect of degree of intermolecular hydrogen bonding by odd-even parity and steric repulsion of neighboring alkyl chains possibly brought the variations in thermochromic response.

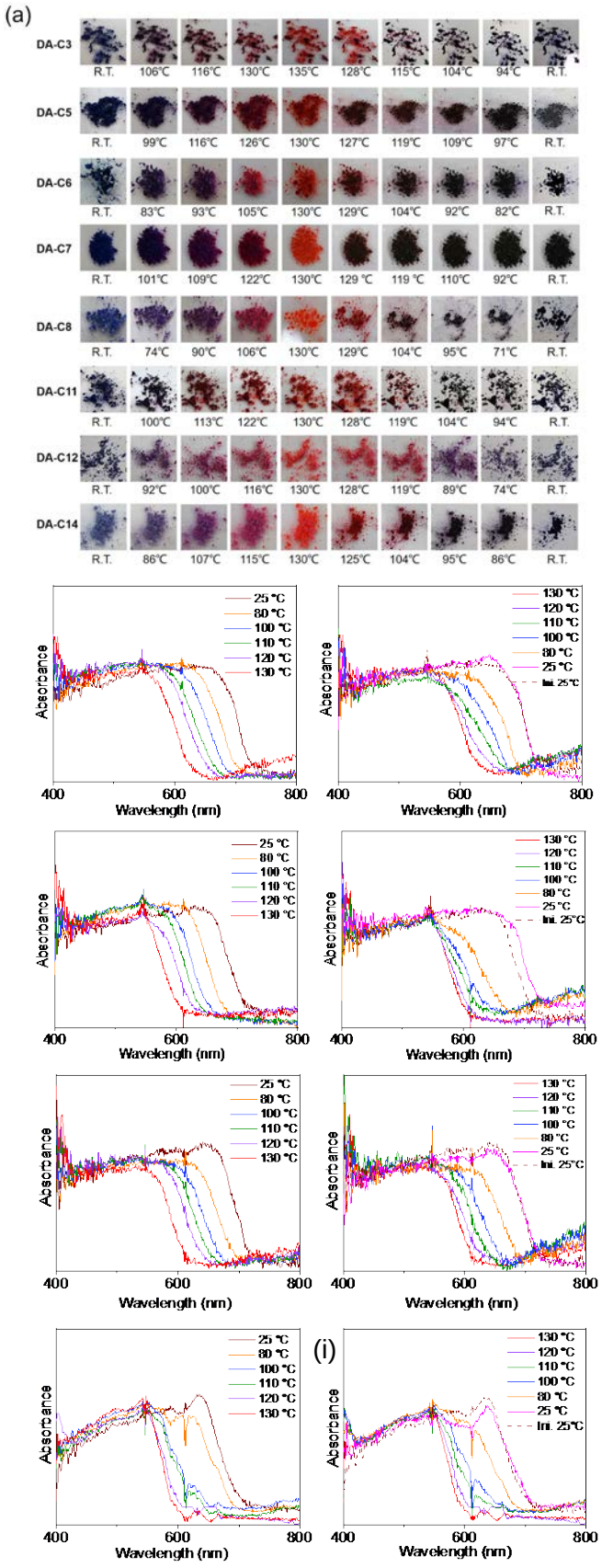

Figure 6 (a) Photos of thermochromic behavior of PDAs between PDA_{blue} and PDA_{red} states upon thermal treatment followed by cooling to RT. (b~i) UV-vis absorption spectra of PDAs monitored at each temperature upon heating and subsequent cooling. PDA n=5 (b: heating, c: cooling), n=6 (d: heating, e: cooling), n=7 (f: heating, g: cooling) and n=8 (h: heating, i: cooling).

Conclusion

In summary, we synthesized a series of bisamide-substituted DAs with varying terminal alkyl spacers, and their molecular structural effect on the unique photopolymerizability of DAs in response to the applied pressure as well as thermochromic properties of PDAs were systematically investigated. The terminal alkyl spacer length, especially its odd-even parity plays a key role to determine the intrinsic intermolecular hydrogen bonding nature of DA crystals and resultant molecular packing. Meanwhile, mechano-responsive crystalline phase transitions exhibiting photopolymerization were valid for all bisamide-substituted DA derivatives regardless of their alkyl spacer length. In this study, we demonstrated that the photopolymerization ability of DAs can be rather simply tuned by changing terminal alkyl length. It would considerably save the effort and expense of synthesizing a series of DAs for different purposes that are selectively responsive to either pressure or light. In addition, the odd-even parity effect was also observed from the distinctive variations in thermochromic behavior of bisamide-substituted PDAs switching between blue, purple, red and orange phases which permits its application for patternable temperature sensors.

Experimental Section

Materials: 10,12-docosadiynedioic acid was purchased from Alfa Aesar, and alkylamines (n = 3, 5, 6, 7, 8, 11, 12 and 14) were purchased from Aldrich. N,N-Diisopropylethylamine and oxalyl chloride were obtained from Wako Chemicals and TCI Chemicals, respectively. 1-Ethyl-3-(3-dimethylaminopropyl)carbodiimide hydrochloride (WSCI · HCl) Watanabe Chemicals. All purchased chemicals were used as obtained without further purification.

Synthesis of bisamide-substituted DA derivatives: DA n = 8 and 14 were synthesized and confirmed according to our previous report.[13] Other DA derivatives were synthesized by either synthetic route-1 or route-2 as described below.

Synthetic route-1: 10,12-Docosadiyndioic acid (0.7 g, 2mmol) was added to a solution of alkylamine (10 mmol) in dichloromethane (40 mL). After WSCI HCl (1.9 g, 10 mmol) and a catalytic amount of N,N-diisopropylethylamine were added, the reaction mixture was stirred for one day at room temperature. Then, it was washed with 1 M HCl, saturated sodium bicarbonate solution, and deionized water. The organic layer was dried over magnesium sulfate. The compound was purified by recrystallization after filtration and the evaporation of solvent. It was dissolved into chloroform upon heating, and then slowly added to a hot butanone (MEK). After cooling to room temperature, the formed crystallites were filtered and dried under vacuum.

Synthetic route-2: To a solution of 10,12-docosadiyndioic acid (0.5 g, 1.4 mmol) in chloroform 25 mL, oxalyl chloride (0.65 g, 5.1 mmol) was added dropwise for 20 min followed by adding a catalytic amount of dimethylformamide (DMF). The reaction mixture was stirred for 12 h at room temperature. To a solution of alkylamine (3 equiv) and triethylamine (1.2 g, 9 equiv) in chloroform, the resultant reaction mixture was added dropwise and then stirred for one day. The final compound was purified with the same recrystallization method described above.

Dipropyldocosa-10,12-diynediamide (n=3): By the route-1 with 10,12-docosadiyndioic acid (0.7 g, 2 mmol) and propylamine (0.6 g, 10 mmol), the final compound was collected as white solid (0.49 g, 53%). ^{1}H NMR (400 MHz, $CDCl_3$): δ = 5.42 (s, 2H), 3.27 – 3.09 (q, 4H), 2.22 (t, J = 7.0 Hz, 4H), 2.17 – 2.10 (m, 4H), 1.71 – 1.10 (m, 28H), 0.90 (t, J = 7.4 Hz, 6H). ^{13}C NMR (100 MHz, $CDCl_3$): δ= 173.12, 77.09, 65.35, 41.23, 36.98,

29.25, 29.23, 28.96, 28.33, 25.86, 23.00, 19.25, 11.44. MALDI-TOF-MS *m/z*: found 445.44 (calcd $[M]^+$ = 445.37). Melting point: 128 ˚C.

Dipentyldocosa-10,12-diynediamide (n=5): By the route-2 with 10,12-docosadiyndioic acid (0.5 g, 1.4 mmol) and amylamine (0.38 g, 3 equiv), the final compound was collected as white solid (0.34 g, 49%). ^{1}H NMR (400 MHz, $CDCl_3$): *δ* = 5.44 (s, 2H), 3.24 (dd, *J* = 5.7, 1.4 Hz, 4H), 2.33 – 2.19 (m, 4H), 2.19 – 2.02 (m, 4H), 1.69 – 1.20 (m, 36H), 0.90 (m, 6H). ^{13}C NMR (100 MHz, $CDCl_3$): *δ*= 173.09, 77.10, 65.36, 39.55, 36.99, 29.46, 29.29, 29.25, 29.15, 28.98, 28.82, 28.35, 25.87, 22.45, 19.26, 14.08. MALDI-TOF-MS *m/z*: found 501.48 (calcd $[M]^+$ = 501.44). Melting point: 121 ˚C.

Dihexyldocosa-10,12-diynediamide (n=6): By the route-1 with 10,12-docosadiyndioic acid (0.7 g, 2 mmol) and hexylamine (1.01 g, 10 mmol), the final compound was obtained as white solid (0.25 g, 23%). ^{1}H NMR (400 MHz, $CDCl_3$): δ 5.39 (s, 2H), 3.22 (dd, J = 13.2, 7.0 Hz, 4H), 2.22 (t, J = 7.0 Hz, 4H), 2.13 (t, J = 7.6 Hz, 4H), 1.67 – 1.16 (m, 40H), 0.87 (t, J = 6.5 Hz, 6H). ^{13}C NMR (100 MHz, $CDCl_3$): *δ*= 173.08, 77.10, 65.36, 39.58, 36.99, 31.57, 29.73, 29.27, 28.98, 28.35, 26.67, 25.87, 22.64, 19.26, 14.10. MALDI-TOF-MS *m/z*: found 529.47 (calcd $[M]^+$ = 529.47). Melting point: 120 ˚C.

Diheptyldocosa-10,12-diynediamide (n=7): By the route-2 with 10,12-docosadiyndioic acid (0.5 g, 1.4 mmol) and heptylamine (0.49 g, 3 equiv), the final compound was collected as white solid (0.35 g, 54%).^{1}H NMR (400 MHz, $CDCl_3$): *δ* = 5.44 (s, 2H), 3.25 (dd, *J* = 7.0, 1.1 Hz, 4H), 2.25 (t, *J* = 7.0 Hz, 4H), 2.21 – 2.11 (m, 4H), 1.64 – 1.17 (m, 44H), 0.89 (t, *J* = 6.9 Hz, 6H). ^{13}C NMR (100 MHz, $CDCl_3$): *δ*= 173.07, 77.09, 65.35, 39.58, 37.00, 31.83, 29.77, 29.29, 29.25, 29.04, 28.98, 28.34, 26.96, 25.87, 22.67, 19.26, 14.15. MALDI-TOF-MS *m/z*: found 557.50 (calcd $[M]^+$ = 557.50). Melting point: 123 ˚C.

Diundecyldocosa-10,12-diynediamide (n=11): By the route-2 with 10,12-docosadiyndioic acid (0.5 g, 1.4 mmol) and 1-aminoundecane (0.74 g, 3 equiv), the final compound was collected as white solid (0.19 g, 20%). ^{1}H NMR (400 MHz, $CDCl_3$): *δ* = 5.39 (s, 2H), 3.28 – 3.16 (m, 4H), 2.23 (d, *J* = 6.1 Hz, 4H), 2.13 (s, 4H), 1.40 (dd, *J* = 106.1, 26.0 Hz, 60H), 0.89 (m, 6H). ^{13}C NMR (100 MHz, $CDCl_3$): *δ*= 178.21, 77.09, 64.31, 37.00, 31.98, 29.77, 29.67, 29.63, 29.41, 29.39, 29.24, 28.98, 28.82, 27.00, 25.86, 22.77, 14.19. MALDI-TOF-MS *m/z*: found 691.65 (calcd $[M + Na]^+$ = 691.62). Melting point: 124 ˚C.

Didodecyldocosa-10,12-diynediamide (n=12): By the route-2 with 10,12-docosadiyndioic acid (0.5 g, 1.4 mmol) and dodecylamine (1.85 g, 10 mmol), the final compound was collected as white solid (0.35 g, 36%). ^{1}H NMR (400 MHz, $CDCl_3$) δ 5.43 (s, 2H), 3.26 (dd, *J* = 13.7, 6.7 Hz, 4H), 2.26 (t, *J* = 6.9 Hz, 4H), 2.20 – 2.07 (m, 4H), 1.59 – 1.14 (m, 64H), 0.90 (t, *J* = 6.8 Hz, 6H). ^{13}C NMR (100 MHz, $CDCl_3$): *δ*= 172.94, 77.10, 65.36, 32.00, 31.03, 29.74, 29.72, 29.64, 29.44, 29.39, 28.99, 22.78, 14.21. MALDI-TOF-MS *m/z*: found 697.70 (calcd $[M]^+$ = 697.66). Melting point: 122 ˚C.

Equipment and methods: ^{1}H NMR spectra were measured with a JEOL JNM-ECX 400 spectrometer and all chemical shifts are quoted in ppm relative to the signal of tetramethylsilane (δ = 0.00) as an internal standard. ^{13}C NMR spectra were measured with a JEOL JNM-ECX 400 spectrometer and all chemical shifts (δ) are quoted in ppm using residual solvents of $CDCl_3$ (δ = 77.16) as the internal standard. Matrix-assisted laser desorption ionization time-of-flight (MALDI-TOF) mass spectra were recorded on an AB SCIEX TOF/TOF 5800. Absorption spectra of PDA powders at each temperature during heating or cooling on the hot plate (AS ONE, digital hot plate Ninos ND-1A) were recorded using SEC2021 Spectrometer (ALS Co. Ltd) equipped with a reflective optical fiber probe (Ocean Optics, Inc.). UV-light irradiation for photopolymerization was carried out using a hand-held UV lamp (AS ONE, model Handy UV Lamp SLUV-4) with a wavelength of 254 nm (0.6 mW/cm^2). Pristine DA powders recrystallized in MEK[13] were fully dried under vacuum at room temperature before use. The mechanical force of 50 MPa was applied for 1 minute to the pristine DA powders by the manual hydraulic pump utilizing a manual table press (NPa System Co., Ltd., model TB-200H-OH300) and a pressure vessel (NPa System Co., Ltd., model CPP35-200B). Powder XRD measurements were carried out with a Rigaku SmartLab. The DSC measurements were carried out using a Hitachi DSC 7020 with a heating/cooling rate of 2 ˚C/min under nitrogen atmosphere. FT-IR and Raman spectroscopy were measured with FT-IR6100 (Jasco Inc) by the ATR method and inVia Reflex Raman spectrometer (Renishaw plc.), respectively.

Crystallography: The diffraction data for DA n=8 was recorded on a DECTRIS EIGER X 1M Detector System (λ = 0.78263°) at 200 K at Spring-8 BL40XU. The diffraction images were processed by using RIGAKU RAPID AUTO.[27] The structures were solved by direct methods (SHELXT-2015[28]) and refined by full-matrix least squares calculations on F_2 (SHELXL-2015)[28] using the Olex2[29] program package. The crystallographic data is summarized in Table S1 (ESI). CCDC 2038568 contains the supplementary crystallographic data for this paper.

Acknowledgements

N. T. gratefully acknowledges financial support from Ogasawara Toshiaki Memorial Foundation. This work was partially supported by the Cooperative Research Program of the Network Joint Research Center for Materials and Devices from the Ministry of Education, Culture, Sports, Science and Technology (MEXT) and the Dynamic Alliance for Open Innovation Bridging Human, Environment and Materials from MEXT. Crystallographic data were collected using synchrotron radiation at the BL40XU in the SPring-8 with approval of JASRI (proposal no. 2018B1244).

Keywords: diacetylene • mechanoresponsive • odd-even parity • polydiacetylene • pressure-induced crystalline transition • topochemical polymerization

[1] F. Braunschweig, H. Bassler, *Chem. Phys.* **1985**, *93*, 307-318.
[2] J. Li, C. Nagamani, J. S. Moore, *Acc. Chem. Res.* **2015**, *48*, 2181-2190.
[3] L. M. de Espinosa, W. Meesorn, D. Moatsou, C. Weder, *Chem. Rev.* **2017**, *117*, 12851- 12892.
[4] A. P. Haehnel, Y. Sagara, Y. C. Simon, C. Weder, *Top. Curr. Chem.* **2015**, *369*, 345-375.
[5] J. Ribas-Arino, M. Shiga, D. Marx, *J. Am. Chem. Soc.* **2010**, *132*, 10609-10614.
[6] H. Feng, J. Lu, J. Li, F. Tsow, E. Forzani, N. Tao, *Adv. Mater.* **2013**, *25*, 1729-1733.
[7] G. N. Patel, R. R. Chance, E. A. Turi, Y. P. Khanna, *J. Am. Chem. Soc.* **1978**, *100*, 6644-6649.
[8] X. Sun, T. Chen, S. Huang, L. Li, H. Peng, *Chem. Soc. Rev.* **2010**, *39*, 4244-4257.
[9] Y. Yao, H. Dong, F. Liu, T. P. Russell, W. Hu, *Adv. Mater.* **2017**, *29*, 1701251
[10] H. Matsuzawa, S. Okada, A. Sarkar, H. Matsuda, H. Nakanishi, *Polymer J* **2001**, *33*, 182-189.
[11] C. Wilhelm, S. A. Boyd, S. Chawda, F. W. Fowler,N. S. Goroff, G. P. Halada, C. P. Grey, J. W. Lauher, L. Luo, C. D. Martin, J. B. Parise, C. Tarabrella, J. A. Webb, *J. Am. Chem. Soc.* **2008**, *130*, 4415-4420.
[12] H. Jin, A. M. Plonka, J. B, Parise, N. S. Goroff, *CrystEngComm* **2013**, *15*, 3106-3110.
[13] Y. Kim, K. Aoki, M. Fujioka, J. Nishii, N. Tamaoki, *ACS Appl. Mater. Interfaces* **2018**, *10*, 36407-36414.
[14] S. Ampornpun, S. Montha, G. Tumcharern, V. Vchirawongkwin, M. Sukwattanasinitt, S. Wacharasindhu, *Macromolecules* **2012**, *45*, 9038-9045.

[15] M. J. Kim, S. Angupillai, K. Min, M. Ramalingam, Y. A. Son, *ACS Appl. Mater. interfaces* **2018**, *10*, 24767-24775.
[16] N. Fujita, Y. Sakamoto, M. Shirakawa, M. Ojima, A. Fuji, M. Ozaki, S. Shinkai, *J. Am. Chem. Soc.* **2007**, *129*, 4134-4135.
[17] H. Tachibana, R. Kumai, N. Hosaka, Y. Tokura, *Chem. Mater.* **2001**, *13*, 155-158.
[18] K. Aoki, M. Kudo, N. Tamaoki, *Org. Lett.* **2004**, *6*, 4009-4012.
[19] X. M. Qian, B. Stadler, *Chem. Mater.* **2019**, *31*, 1196-1222.
[20] S. Spagnoli, M. R. Vilar, M. Schott, *Vibration. Spectroscopy* **2014**, *70*, 89-99.
[21] G. A. Jeffrey, Frye in *An Introduction of Hydrogen Bonding,* Oxford University Press, Inc., New York, **1997**, pp. 11.
[22] R. H. Baughman, *J. Polym. Sci. Polym. Phys. Ed.* **1974**, *12*, 1511-1535.
[23] C.-W. Tseng, D.-C. Huang, H.-L. Yang, H.-C. Lin, F.-C. Li, C.-W. Pao, Y.-T. Tao, *Chem. Eur. J.* **2020**, *26*, 13948
[24] C. Tanioku, K. Matsukawa, A. Matsumoto, *ACS Appl. Mater. Interfaces* **2013**, *5*, 940-948.
[25] I. S. Park, H. J. Park, W. Jeong, J. Nam, Y. Kang, K. Shin, H. Chung, J.-M. Kim, *Macromolecules*, **2016**, *49*, 1270-1278.
[26] C. Phollookin, S. Wacharasindhu, A. Ajavakom, G. Tumcharern, S. Ampornpun, T. Eaidkong, M. Sukwattanasinitt, *Macromolecules*, **2010**, *43*, 7540-7548.
[27] RAPID-AUTO manual. Rigaku Corporation, Tokyo, Japan (2001)
[28] G. M. Sheldrick, *Acta Cryst. A* **2015**, *71*, 3-8.
[29] O. V. Dolomanov, L. J. Bourhis, R. J. Gildea, J. A. K. Howard, H. J. Puschmann, *Appl. Cryst.* **2009**, *42*, 339-341.

Entry for the Table of Contents

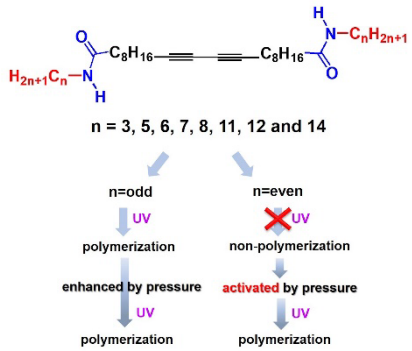

A series of bisamide-substituted diacetylenes with varying terminal alkyl spacer length showed unique pressure-induced photopolymerizability. Odd-and even-parity of terminal alkyl exhibited a light-active and light-inert pristine state, respectively. We revealed that the intermolecular H-bonds were highly influenced by the terminal alkyl parity resulting in the different crystalline packings and photopolymerization properties.